

EUROPEAN ORGANIZATION FOR NUCLEAR RESEARCH

Proposal to the ISOLDE and Neutron Time-of-Flight Committee

Collinear resonance ionization spectroscopy of radium ions

May 30, 2014

K.M. Lynch¹, J. Billowes², M.L. Bissell¹, I. Budinčević¹, T.E. Cocolios²,
T. Day Goodacre^{2,3}, R.P. de Groot¹, V.N. Fedosseev³, K.T. Flanagan², S. Franchoo⁴,
R.F. Garcia Ruiz¹, H. Heylen¹, T. Kron⁵, B.A. Marsh³, G. Neyens¹, R.E. Rossel^{3,5,6},
S. Rothe³, I. Strashnov², H.H. Stroke⁷, K.D.A. Wendt⁵.

¹*KU Leuven, Instituut voor Kern- en Stralingsfysica, B-3001 Leuven, Belgium*

²*School of Physics and Astronomy, The University of Manchester, Manchester, M13 9PL, UK*

³*EN Department, CERN, CH-1211 Geneva 23, Switzerland*

⁴*Institut de Physique Nucléaire d'Orsay, F-91406 Orsay, France*

⁵*Institut für Physik, Johannes Gutenberg-Universität Mainz, D-55128 Mainz, Germany*

⁶*Hochschule RheinMain, Fachbereich Design Informatik Medien, D-65197 Wiesbaden, Germany*

⁷*Department of Physics, New York University, NY, New York 10003, USA*

Spokesperson and Local Contact: Kara M. Lynch (kara.marie.lynch@cern.ch)

Abstract: We propose to study the neutron-deficient radium isotopes with high-resolution collinear resonance ionization spectroscopy. Probing the hyperfine structure of the $7s\ ^2S_{1/2} \rightarrow 7p\ ^2P_{1/2}$ and $7s\ ^2S_{1/2} \rightarrow 7p\ ^2P_{3/2}$ transitions in Ra II will provide atomic-structure measurements that have not been achieved for $A < 208$ Ra.

Measurement of the $7s\ ^2S_{1/2} \rightarrow 7p\ ^2P_{3/2}$ transition in $A < 214$ Ra will allow the spectroscopic quadrupole moments to be directly measured for the first time. In addition, the technique will allow tentative spin assignments to be confirmed and the magnetic dipole moments measured for $A < 208$ Ra. Measurement of the hyperfine structure (in particular the isotope shifts) of the neutron-deficient radium will provide information to further constrain the nuclear models away from the N=126 shell closure.

Requested shifts: 18 shifts

1 Introduction

We propose to study the hyperfine structure of the neutron-deficient radium isotopes with the CRIS beam line [1–3], by probing the atomic structure of the radium ion [4–7]. Scanning the frequency of the first-step in a three-step resonant ionization scheme, the nuclear spins, isotope shifts and electromagnetic moments of $^{A<214}\text{Ra}$ can be determined. An overview of the current information available for these isotopes is shown in Table 1. The first transition to be studied ($7s\ ^2S_{1/2} \rightarrow 7p\ ^2P_{1/2}$) will provide new information on the isotopes $^{A<208,209}\text{Ra}$ through measurement of their magnetic moments, and thus their nuclear configuration. Studying the second transition ($7s\ ^2S_{1/2} \rightarrow 7p\ ^2P_{3/2}$) will allow the spectroscopic quadrupole moments of $^{A<208,213}\text{Ra}$ to be measured for the first time, as well as confirming the tentative spin assignments. The study of the neutron-deficient radium isotopes is crucial for providing important information to test the validity of theoretical nuclear models away from the N=126 shell closure [8], in addition to providing atomic-structure information for atomic parity non-conservation measurements [9]. In particular, the charge-radii of even-Z nuclei have been shown to be sensitive observables to challenge beyond-mean-field calculations [10–13].

Table 1: An overview of the current information available for the neutron-deficient radium isotopes. *Calculation from a semi-empirical analysis of the hyperfine structure of Ra I, not directly measured.

A	N	I	μ (μ_N) [14]	Q_s (b) [15]	$\delta\nu$ [15, 16]	
					$7s\ ^2S_{1/2} \rightarrow 7p\ ^2P_{1/2}$	$7s\ ^2S_{1/2} \rightarrow 7p\ ^2P_{3/2}$
214	126	0 ⁺			✓	✓
213	125	1/2 ⁻	0.6133(18)	✗	✓	
212	124	0 ⁺			✓	✓
211	123	5/2 ⁽⁻⁾	0.8780(38)	0.48(6)*	✓	
210	122	0 ⁺			✓	
209	121	5/2 ⁻	0.865(13)	0.40(6)*		
208	120	0 ⁺			✓	
207	119	(3/2 ⁻ , 5/2 ⁻)				
206	118	0 ⁺				
205	117	(3/2 ⁻)				

With the high sensitivity provided by ion detection coupled with the high-resolution inherent to the collinear laser spectroscopic method, collinear resonance ionization spectroscopy (CRIS) can measure the hyperfine structure of these more exotic isotopes. With measurements of the hyperfine structure of isotopes with yields of 100 atoms/s already achieved with ^{202}Fr [$t_{1/2}=0.30$ s], it is estimated that the neutron-deficient radium isotopes down to ^{205}Ra [$t_{1/2}=0.21$ s] can be studied.

2 Physics motivation

With the CRIS beam line, we propose to study the hyperfine structure of both the $7s\ ^2S_{1/2} \rightarrow 7p\ ^2P_{1/2}$ (468.2 nm) and $7s\ ^2S_{1/2} \rightarrow 7p\ ^2P_{3/2}$ (381.4 nm) transitions in Ra II.

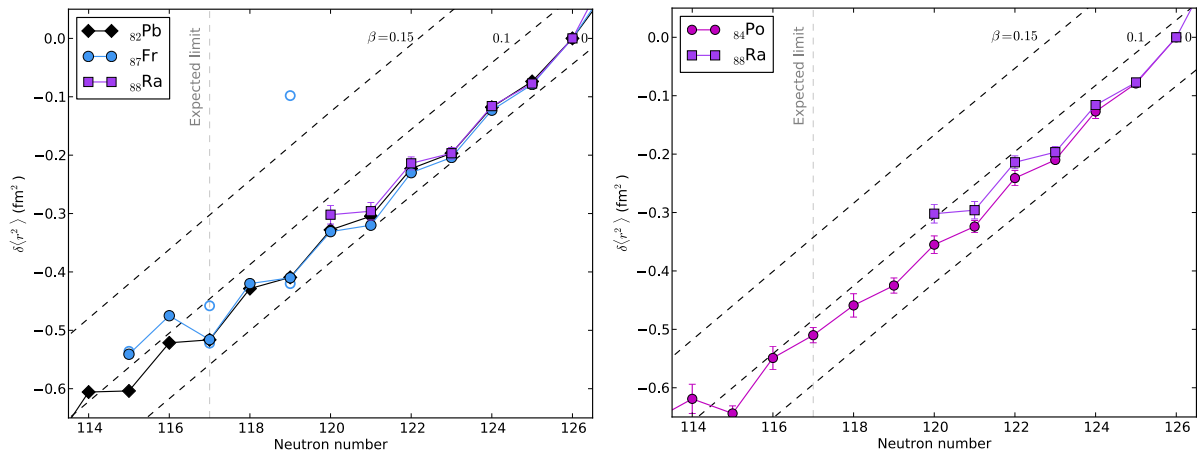


Figure 1: (Left) Overlaid relative mean-square charge radii of ^{82}Pb (diamonds) [18], ^{87}Fr (circles) [19–21] and ^{88}Ra (squares) [14] isotopes[†]. The value for $^{202}\text{Fr}_{115}$ represents the current detection limit of the CRIS experiment (100 atoms/s). The grey dashed line represents the expected measurement limit of this campaign. (Right) Overlaid relative mean-square charge radii of ^{84}Po (circles) [12, 22, 23] and ^{88}Ra (squares) [14] isotopes[‡]. The departure from sphericity (prominent in the Po isotopes at N=114) is thought to occur earlier for Ra isotopes.

A detailed knowledge of these transitions will provide not only useful measurements of the atomic structure of radium, but will provide the information to understand radium in a nuclear-structure framework [17].

Measurement of the $7s\ ^2S_{1/2} \rightarrow 7p\ ^2P_{1/2}$ transition will allow measurement of magnetic-moment values that will provide the nuclear configurations of the odd-A Ra isotopes that are presently unconfirmed. The only neutron-deficient Ra II isotopes to be studied with the $7s\ ^2S_{1/2} \rightarrow 7p\ ^2P_{3/2}$ transition are $^{212,214}\text{Ra}$ [15]. Studying the isotopic radium chain with this transition will allow the hyperfine B factor to be measured and the spectroscopic quadrupole moment determined for $^{A<208,213}\text{Ra}$ for the first time. Using the extracted hyperfine A factor from the $7s\ ^2S_{1/2} \rightarrow 7p\ ^2P_{1/2}$ transition, the fit for the $7s\ ^2S_{1/2} \rightarrow 7p\ ^2P_{3/2}$ transition can be further constrained, allowing a more accurate determination of the B factor, and thus the quadrupole moment. A direct measurement of the quadrupole moment will provide important information on the deformation of the odd-A isotopes as the N=126 shell is depleted. Until now, the only calculation of the quadrupole moments ($^{209,211}\text{Ra}$) have come from a semi-empirical analysis of the hyperfine structure of the $7s7p\ ^3P_J$ configuration in atomic radium (for which the spin is assumed) [15, 16]. Measuring the $7s\ ^2S_{1/2} \rightarrow 7p\ ^2P_{3/2}$ transition in the alkali-like radium ion will provide a more accurate determination of the quadrupole moment, as the single electron simplifies the calculation of the electric field gradient. In addition, this transition will allow unambiguous determination the spin of the $^{A<214}\text{Ra}$ isotopes that are only tentatively assigned (e.g. $^{205,207}\text{Ra}$).

New *ab-initio* many-body calculations for the low-lying levels in Ra II [8] have provided a

[†]The β -lines for Fr are normalised using $\beta_2(^{213}\text{Fr})=0.062$, evaluated from $E(2_1^+)$ in ^{212}Rn [24, 25].

[‡]The β -lines for Po are normalised using $\beta_2(^{208}\text{Po})=0.086$, evaluated from $E(2_1^+)$ in ^{208}Po [24, 25].

more accurate determination of the field and specific mass shifts for the transitions under investigation. By measuring the relative charge radii of $^{A < 208}\text{Ra}$ and the quadrupole moments of $^{A < 214}\text{Ra}$, a thorough investigation into the deformation of these neutron-deficient nuclei can be achieved. The charge radii of radium measured so far display a surprising agreement with those of the magic $_{82}\text{Pb}$ nuclei, shown in Figure 1 (left), despite the 6 valence-protons difference [16]. Similarly, the $_{87}\text{Fr}$ isotopes (with their 5 valence protons) only deviate from the Pb trend at ^{203}Fr due to the onset of collectivity [20]. In order to separate the contribution of the even- Z core from the independent proton particle, a detailed study of the radon and radium neighbours of francium is required. The deformed (10^-) state observed in ^{206}Fr [$t_{1/2}=0.7$ s] [21], shown in Figure 1 (left), occurs at an excitation energy of only 531 keV. The experiment to measure the quadrupole moment of this state, and determine its static deformation, has already been endorsed by the INTC [26]. In the single-particle approximation, the isomeric states of $^{205,207}\text{Ra}$ ($13/2^-$) occur from the same neutron excitation as that of the (10^-) state in ^{206}Fr (forming a hole in the $\nu(i_{13/2})$ shell). Using the alpha-tagging technique available at CRIS, the isomeric states in radium can be studied, and the interplay between the single-particle and collective nature of the states investigated. A future experiment on the neutron-deficient radon isotopes is thus envisaged, in order to extend the nuclear structure measurements above the $Z=82$ shell closure, and fully characterise this region.

Figure 1 (right) presents the relative charge-radii of radium alongside those of the $_{84}\text{Po}$ isotopes. The departure from sphericity observed at $N=114$ in polonium [12,23] is expected to occur closer to $N=126$ with increasing Z [27,28]. By measuring the isotope shifts towards ^{205}Ra ($N=117$), it can be determined if the charge radii of the radium isotopes follow the same trend as that of francium and radon, or if an earlier departure from sphericity occurs. Comparison with the charge-radii from beyond-mean-field calculations [10,29] will allow a deeper understanding of the experimental results. Relativistic-mean-field approaches give a good description of the charge radii, where beyond-mean-field correlations have been seen to have a very small effect on the heavy nuclei close to $N=126$ [10]. Studying nuclei further from this shell closure (with $N < 126$) will provide a rigorous test for this model, while providing information on the deformation of the energy surface. Studying the radium isotopes (with their protons occupying high- j orbitals) will test the suggestion that this causes a softness in the deformation energy surface, causing shape coexistence [12]. Beyond-mean-field calculations suggest the departure of polonium from the Pb trend is due to a softening of their deformation energy surface, but they remain essentially spherical [12]. This is not supported by recent quadrupole-moment measurements that show that the ground state is statically deformed [23]. Studying the quadrupole moments of the radium isotopes is critically important in order to understand any departure from the Pb trend in terms of static deformation.

The recent measurements of the isotope shifts of Ra II have arisen from a desire for a detailed knowledge of the atomic structure of radium to aid atomic parity non-conservation (APNC) tests [30,31]. The atomic structure of the $7s\ ^2S_{1/2}$ ground state and the metastable $6d\ ^2D_{3/2}$ state are of particular importance due to the planned experiment to measure parity non-conservation at the KVI of the University of Groningen [32]. An

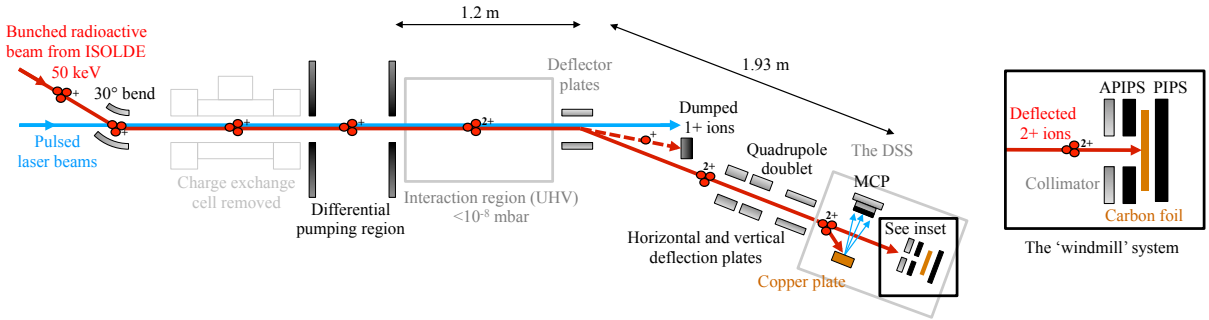


Figure 2: Schematic diagram of the CRIS beam line. Resonant 2^+ ions can be deflected to a copper plate and the corresponding secondary electrons detected by the MCP, or (Inset) implanted into a carbon foil for alpha-decay spectroscopy.

atomic test of the standard model, APNC gives rise to a small parity-nonconserving electric dipole transition amplitude ($E1_{PNC}$) that will be measured in the $7s\ 2S_{1/2} \rightarrow 6d\ 2D_{3/2}$ transition with a singly-trapped radium ion [33].

This planned experiment in Groningen has motivated the recent study into the charge radii of the radium isotopes, using *ab-initio* many-body calculations to provide new values for the field shifts and specific mass shifts of the neighbouring levels in Ra II [8]. This study used the initial experimental results of the hyperfine-structure studies of radium performed by the ISOLDE collaboration in the 1980's [15,16,34] alongside the more recent experimental data [30–32]. In the case of the ISOLDE experiment, the combination of low yield and short lifetimes for isotopes under investigation resulted in low signal-to-noise ratios that left the radium isotopes $A < 208$ Ra unable to be measured, and the study of the neutron-deficient isotopes incomplete. By taking advantage of the new calculations available and utilising the sensitivity inherent to ion detection, the CRIS technique provides the opportunity to study these neutron-deficient radium isotopes.

3 Experimental method

The radium isotope of interest is mass-selected using the high-resolution HRS separator, bunched with the radio-frequency cooler-buncher ISCOOL and deflected into the CRIS beam line [35], see Figure 2. The bunching of the beam with ISCOOL is essential to match the duty cycle of the pulsed laser system used. The bunched ion beam is then transported through the CRIS beam line into the interaction region. The charge exchange cell is removed to allow resonance ionization to occur in Ra II. Ion-ionization is preferred over ionizing the atom to avoid neutralization into a metastable state of the atom [36,37] when passed through the charge-exchange cell (populating a state that is inaccessible to the laser light e.g. $7s6d\ 3D_3$). Resonantly exciting from the $7s\ 2S_{1/2}$ state will provide an accessible 50% population in both hyperfine levels. In addition, the transmission efficiency of the beam will increase, due to the removal of the small apertures in the charge-exchange cell.

In the 1.2 m interaction region, the arrival of the ion bunch (temporal length of $\sim 5\ \mu\text{s}$)

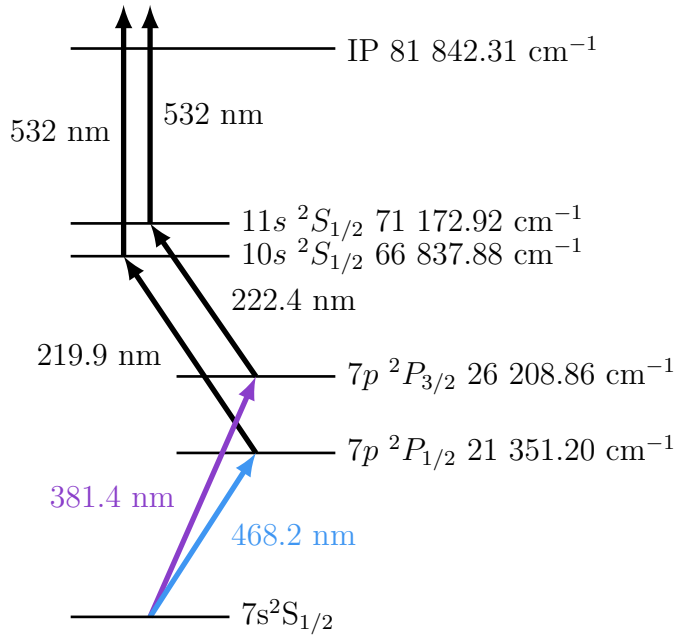


Figure 3: The two proposed three-step resonance ionization schemes for Ra II. By measuring both transitions, the hyperfine parameters extracted from the first transition (A factor) can further constrain those extracted from the second transition (B factor), providing more reliable quadrupole-moment values.

is synchronized with three co-propagating pulsed laser beams to step-wise excite and ionize the state of interest. The resonance-ionization schemes for the Ra II isotopes are shown in Figure 3. The hyperfine structure of the first resonant-excitation step (of the three-step scheme) will be probed by scanning the frequency of the first-step laser, produced by frequency-doubling light from a CW Ti:Sa laser. A broadband second-step (frequency-tripled light from a pulsed-dye laser) and brute-force third step into the continuum (frequency-doubled light from a Nd:YAG laser) will doubly ionize the Ra II ion. Reduction of the background signal (resulting from non-resonant collisional ionization) is expected to significantly decrease due to the low cross-section of the double-ionization method needed to produce Ra III. However, in order to minimize this process it is required that the interaction region operates in ultra-high vacuum conditions. The setup has achieved a pressure of $\sim 10^{-10}$ mbar successfully.

After resonance ionization, the Ra III ions are deflected to a copper dynode housed in the decay spectroscopy station (DSS) and the corresponding secondary electrons are detected by an MCP. A full description of the DSS can be found in Ref [38]. In addition to hyperfine-structure studies with ion detection, the DSS can be used to identify the hyperfine components of overlapping structures with the installed silicon detectors [39]. This allows the overlapping hyperfine structure of two (or more) states to be separated by exploiting their characteristic alpha decay. This will be utilised to identify the neutron-deficient radium isotopes that have long-lived isomeric states (^{207}Ra [$t_{1/2}= 59$ ms] and ^{205}Ra [$t_{1/2}=170$ ms]). Until now, the alpha-decay spectroscopy data has been acquired with the ISOLDE digiDAQ, consisting of XIA digital gamma finder (DGF) revision D modules [40]. However, a new data acquisition system is currently under procurement.

Scanning the frequency of the first resonant-excitation step probes the hyperfine structure of the isotope under investigation. From the atomic hyperfine structure, determination of the nuclear observables (spin, magnetic moment, quadrupole moment and isotope shift) is achieved without introducing any assumptions associated with a particular nuclear model [41].

4 Beam time request

We would like to request the following radioactive beams to measure the hyperfine structure of both the $7s\ ^2S_{1/2} \rightarrow 7p\ ^2P_{1/2}$ and $7s\ ^2S_{1/2} \rightarrow 7p\ ^2P_{3/2}$ transitions. This will provide nuclear spins, magnetic dipole moments, electric quadrupole moments and isotope shift measurements. A schematic illustration of the previous measurements alongside the measurements requested in this proposal are shown in Figure 4. A break-down of the requested shifts is shown in Table 2.



Figure 4: A schematic illustration of the radium isotopes that have been measured (black) and are requested to be measured (blue, purple). The hyperfine structure of both the (blue, left) $7s\ ^2S_{1/2} \rightarrow 7p\ ^2P_{1/2}$ transition (468.2nm) and the (purple, right) $7s\ ^2S_{1/2} \rightarrow 7p\ ^2P_{3/2}$ transition (381.4 nm) are requested to be measured in this proposal in order to directly measure the magnetic dipole moments for $A < 208$ Ra and quadrupole moments for $A < 214$ Ra for the first time.

Table 2: Expected yield for the neutron-deficient radium isotopes. Reference measurements will be taken with ^{214}Ra as this N=126 isotope is expected to be spherical. *Estimated yield [42].

Isotope	I	$t_{1/2}$	Expected yield (ions/ μC)	Target	Ion source	Shifts
^{225}Ra	$1/2^+$	14.9(2) d	2.6×10^8	U/ThC _x	RILIS development	4
^{214}Ra	0^+	2.46 (3) s	9.0×10^6	U/ThC _x	Re Surface + RILIS	2
^{213}Ra	$1/2^-$	2.73 (5) m	8.0×10^6 *	U/ThC _x	Re Surface + RILIS	0.5
^{212}Ra	0^+	13.0 (2) s	6.5×10^6	U/ThC _x	Re Surface + RILIS	0.5
^{211}Ra	$5/2^{(-)}$	13 (2) s	3.0×10^6 *	U/ThC _x	Re Surface + RILIS	0.5
^{210}Ra	0^+	3.7 (2) s	9.9×10^5	U/ThC _x	Re Surface + RILIS	0.5
^{209}Ra	$5/2^-$	4.6 (2) s	1.5×10^5 *	U/ThC _x	Re Surface + RILIS	0.5
^{208}Ra	0^+	1.3 (2) s	2.5×10^4	U/ThC _x	Re Surface + RILIS	0.5
^{207}Ra	$(3/2^-, 5/2^-)$	$1.35 \begin{smallmatrix} +22 \\ -13 \end{smallmatrix}$ s	3.0×10^3 *	U/ThC _x	Re Surface + RILIS	2
^{206}Ra	0^+	0.24 (2) s	6.0×10^2 *	U/ThC _x	Re Surface + RILIS	3
^{205}Ra	$(3/2^-)$	$0.21 \begin{smallmatrix} +6 \\ -4 \end{smallmatrix}$ s	8.0×10^1 *	U/ThC _x	Re Surface + RILIS	4
Total						18

Four shifts of dedicated beam-time are requested for ionization-scheme development with RILIS. Recent in-source spectroscopy measurements conducted at TRIUMF observed an

increase in the production of radium (compared to surface ionization) by a factor 3 [43]. With the higher power of the ionizing step (532 nm) available with RILIS, a higher factor is envisaged. By increasing the scan range to the visible spectrum, RILIS will be able to search for more bound and auto-ionizing states.

As there are no stable isotopes of radium, three additional shifts (protons on target) are requested prior to the run to tune the experimental setup and optimize the three-step resonance-ionization process at CRIS. It is also requested to have access to the ISOLDE digiDAQ for a few days prior to the experiment to set up and calibrate the data acquisition system for use with the DSS. A new data acquisition is currently under procurement but the ISOLDE digiDAQ will be relied upon as a contingency plan.

Requested shifts: 18 shifts

References

- [1] J. Billowes et al., CERN-INTC-2008-010 INTC-P-240 (2008), CERN, Geneva
- [2] T.J. Procter et al., J. Phys.: Conf. Ser. **381**, 012070 (2012)
- [3] K.M. Lynch et al., J. Phys.: Conf. Ser. **381**, 012128 (2012)
- [4] J. Boulmer et al., J. Phys. B: At. Mol. Opt. Phys. **20**, L143 (1987)
- [5] W. Huang et al., J. Opt. Soc. Am. B **12**, 961 (1995)
- [6] M. Seng et al., Eur. Phys. J. D **3**, 21 (1998)
- [7] O.A. Herrera-Sancho et al., Phys. Rev. A **88**, 012512 (2013)
- [8] L.W. Wansbeek et al., Phys. Rev. C **86**, 015503 (2012)
- [9] L.W. Wansbeek et al., Phys. Rev. A **78**, 050501 (2008)
- [10] M. Bender, G.F. Bertsch, P.H. Heenen, Phys. Rev. C **73**, 034322 (2006)
- [11] H. De Witte et al., Phys. Rev. Lett. **98**, 112502 (2007)
- [12] T.E. Cocolios et al., Phys. Rev. Lett. **106**, 052503 (2011)
- [13] P.M. Goddard et al., Phys. Rev. Lett. **110**, 032503 (2013)
- [14] S. Ahmad et al., Nucl. Phys. A **483**, 244 (1988)
- [15] W. Neu et al., Z. Phys. D **11**, 105 (1988)
- [16] K. Wendt et al., Z. Phys. D **4**, 227 (1987)
- [17] K. Blaum et al., Phys. Scripta **2013**, 014017 (2013)

- [18] M. Anselment et al., Nucl. Phys. A **451**, 471 (1986)
- [19] V.A. Dzuba et al., Phys. Rev. A **72**, 022503 (2005)
- [20] K.T. Flanagan et al., Phys. Rev. Lett. **111**, 212501 (2013)
- [21] K.M. Lynch et al., Phys. Rev. X **4**, 011055 (2014)
- [22] D. Kowalewska et al., Phys. Rev. A **44**, R1442 (1991)
- [23] M. Seliverstov et al., Phys. Lett. B **719**, 362 (2013)
- [24] W.D. Myers, K.H. Schmidt, Nucl. Phys. A **410**, 61 (1983)
- [25] S. Raman, C.N. Jr., P. Tikkanen, Atomic Data and Nuclear Data Tables **78**, 1 (2001)
- [26] K.T. Flanagan et al., CERN-INTC-2014-020 INTC-P-240-ADD-1 (2014), CERN, Geneva
- [27] K. Heyde, J.L. Wood, Rev. Mod. Phys. **83**, 1467 (2011)
- [28] J. Elseviers et al., Phys. Rev. C **84**, 034307 (2011)
- [29] M. Bender, P.H. Heenen, P.G. Reinhard, Rev. Mod. Phys. **75**, 121 (2003)
- [30] O.O. Versolato et al., Phys. Rev. A **82**, 010501 (2010)
- [31] G.S. Giri et al., Phys. Rev. A **84**, 020503 (2011)
- [32] O. Versolato et al., Phys. Lett. A **375**, 3130 (2011)
- [33] O.O. Versolato et al., Can. J. Phys. **89**, 65 (2011)
- [34] S. Ahmad et al., Physics Letters B **133**, 47 (1983)
- [35] T.J. Procter, K.T. Flanagan, Hyperfine Interact. **216**, 89 (2013)
- [36] V.A. Dzuba, V.V. Flambaum, J. Phys. B: At. Mol. Opt. Phys. **40**, 227 (2007)
- [37] W.L. Trimble et al., Phys. Rev. A **80**, 054501 (2009)
- [38] M.M. Rajabali et al., Nucl. Instrum. Methods Phys. Res. A **707**, 35 (2013)
- [39] K.M. Lynch, T.E. Cocolios, M.M. Rajabali, Hyperfine Interact. **216**, 95 (2013)
- [40] W. Hennig et al., Nucl. Instrum. Methods Phys. Res. B **261**, 1000 (2007)
- [41] B. Cheal, K.T. Flanagan, J. Phys. G **37**, 113101 (2010)
- [42] A. Gottberg, *Private communication*
- [43] S. Raeder et al., Hyperfine Interactions **227**, 77 (2014)

Appendix

DESCRIPTION OF THE PROPOSED EXPERIMENT

The experimental setup comprises:

Part of the	Availability	Design and manufacturing
CRIS experiment	<input checked="" type="checkbox"/> Existing	<input checked="" type="checkbox"/> To be used without any modification

HAZARDS GENERATED BY THE EXPERIMENT

Hazards named in the document relevant for the fixed CRIS installation.